Decoding transcriptomic intra–tumour heterogeneity to guide personalised medicine in ovarian cancer

Tuan Zea Tan[1†], Valerie Heong[1,2,3†], Jieru Ye[1], Diana Lim[4,5], Jeffrey Low[6], Mahesh Choolani[6], Clare Scott[3], David Shao Peng Tan[1,2,7] and Ruby Yun-Ju Huang[1,6,8*]

[1]Cancer Science Institute of Singapore, National University of Singapore, Center for Translational Medicine, 14 Medical Drive,MD6 #12-01, Singapore 117599
[2]Department of Haematology-Oncology, National University Cancer Institute Singapore, Level 8 NUH Medical Center, 5 Lower Kent Ridge Road, Singapore 119074
[3]Walter and Eliza Hall Institute of Medical Research, Parkville, Victoria 3052, Australia
[4]Department of Pathology, National University Health System, 1E Kent Ridge Road Singapore 119228
[5]Department of Pathology, Yong Loo Lin School of Medicine, National University of Singapore, 4 Medical Drive, MD4 #04-01, Singapore 117597
[6]Department of Obstetrics and Gynecology, National University Health System, 1E Kent Ridge Road Singapore 119228
[7]Department of Medicine, Yong Loo Lin School of Medicine, National University of Singapore. 1E Kent Ridge Road, NUHS Tower Block, Level 10, Singapore 119228.
[8]Department of Anatomy, Yong Loo Lin School of Medicine, National University of Singapore, 4 Medical Drive, MD4 #04-01, Singapore 117597

[†]Equally contributing authors

Correspondinence to: Ruby Yun-Ju Huang, Cancer Science Institute of Singapore, National University of Singapore, Center for Translational Medicine, 14 Medical Drive, #11-01, Singapore 117599. Phone: +65 6516 1148. E-mail: csihyjr@nus.edu.sg

Running title: Intra-tumour subtype heterogeneity in ovarian cancer.

The authors declare no conflict of interest.

Word count: 4,300.

Abstract

The evaluation of intra-tumour heterogeneity (ITH) from a transcriptomic point of view is limited. Single-cell cancer studies reveal significant genomic and transcriptomic ITH within a tumour and it is no longer adequate to employ single-subtype assignment as this does not acknowledge the ITH that exists. Molecular assessment of subtype heterogeneity (MASH) was developed to comprehensively report on the composition of all transcriptomic subtypes within a tumour lesion. Using MASH on 3,431 ovarian cancer samples, correlation and association analyses with survival, metastasis, and clinical outcomes were performed to assess the impact of subtype composition as a surrogate for ITH. The association was validated on two independent cohorts. We identified that 30% of ovarian tumours consist of two or more subtypes. When biological features of the subtype constituents were examined, we identified significant impact on clinical outcomes with the presence of poor prognostic subtypes (Mes or Stem-A). Poorer outcomes correlated with having higher degrees of poor prognostic subtype populations within the tumour. Subtype prediction in several independent datasets reflected a similar prognostic trend. In addition, paired analysis of primary and recurrent/metastatic tumours demonstrated Mes and/or Stem-A subtypes predominated in recurrent and metastatic tumours regardless of the original primary subtype. Given the biologic and prognostic value in delineating individual subtypes within a tumour, a clinically applicable MASH assay using NanoString technology was developed as a classification tool to comprehensively describe constituents of molecular subtypes.

Introduction

Ovarian cancer (OC) is the sixth leading cause of cancer mortality in developed countries [1]. In 80% of patients with advanced OC, the disease recurs despite optimal surgical cytoreduction and adjuvant systemic platinum-based chemotherapy. At disease recurrence, tumours may be platinum sensitive or resistant, and the spectrum of chemosensitivity may be partially explained by the existence of at least four different histological subtypes—high grade serous (HGSOC), endometrioid, clear cell, and mucinous carcinoma. Histological differences alone, however, cannot fully account for the heterogeneity in clinical outcomes because differences in patient outcomes and responses to chemotherapy also exist between patients with seemingly identical histological subtypes. Therefore, other underlying mechanisms that underpin drug resistance in OC require further exploration. Plausible mechanisms include inter- and intra-tumoural heterogeneity driven by genomic alterations [2-5] or molecular signatures [6,7], and clonal evolution and/or chemoresistant stem cell-like populations in the primary tumour [3,8].

Tothill *et al*, [7] identified six molecular subtypes of HGSOC—with associated biological and clinical significance based on gene expression profiling, which was later validated in several independent studies [6,9]. Similarly, we identified five molecular subtypes based on gene expression profiling [6]. When we compared the subtype definitions from Tothill *et al* [7], TCGA [9], and our previous work [6], we observed significant concordance in molecular features and associated clinical outcomes [6]. The Clinical Proteomic Tumour Analysis Consortium (CPTAC) refined the molecular subtypes by integrating transcriptomics and proteomics [10] which identified a very similar classification system as that described by TCGA, except for a rare subtype "stromal" which was not identified previously. Due to the lack of publicly available proteomics data, and the similarities between the CPTAC and TCGA classification [10], we focused on transcriptomic

molecular subtypes in this study. The 3 transcriptomic molecular subtype definitions are shown in Fig. 1A (subtype in order of Tan *et al* [6]/Tothill *et al* [7]/TCGA[9]): Epithelial-A (Epi-A)/C3/Differentiated, Epithelial-B (Epi-B)/C2/Immunoreactive, Stem-like B (Stem-B)/C6, Mesenchymal (Mes)/C1 and Stem-like A (Stem-A)/C5/Proliferative. The molecular subtypes were correlated with various clinicopathological parameters and showed significant differences in both disease-free survival (DFS) and overall survival (OS) in a univariate analysis [7] as well as in a multivariate Cox regression analysis when taking into account other clinically relevant parameters [6]. Importantly, the Mes/C1 (characterised by elevated pathways of extra-cellular matrix, metastasis, TGF-β signalling) and the Stem-A/C5 (characterized by elevated pathways of chromatin reorganization, WNT signalling, microtubule processing) subtypes were linked to poorer outcomes compared to the other subtypes [6,7]. There is emerging clinical evidence to suggest transcriptomic subtypes can predict therapeutic outcomes in patients with OC. Recent retrospective analysis suggests the addition of bevacizumab to standard chemotherapy conferred a greater benefit in patients with poor prognostic molecular subtypes (Mesenchymal/C1/Mes and proliferative/C5/Stem-A) [11,12]. Accumulating evidence has supported the existence of molecular subtypes, with enrichment of certain genomic and transcriptomic pathways, that exhibit preferential responses to certain cytotoxic agents, such as platinum, paclitaxel, vincristine and vinorelbine [5,6,13,14]. In light of these reports, several gene expression subtype-specific clinical trials have emerged to address the clinical relevance of gene expression signatures in OC.

Conventionally, molecular subtyping deploys a single-subtype assignment to each tumour sample without taking into account the underlying biology of intra-tumour heterogeneity (ITH). ITH has been documented by using single-cell analysis across multiple tumour types including carcinoma of the breast [15], renal [16], lung [17], prostate [18], ovarian [19], glioblastoma [20], melanoma [21], lymphoblastic leukaemia [22] and multiple

myeloma [23]. These studies suggest that the existence of heterogeneity lies not only at the genomic level, but also at the epigenomic and transcriptomic levels. As we expand our taxonomy of tumours and continue to understand the consequences and implications of ITH in solid tumours, it is apparent that a single-subtype annotation is largely inadequate for classifying tumours as it ignores the co-existence of potentially resistant subclones within the tumour [16,18]. While several studies have described the impact of ITH from genomic alterations by using various sequencing approaches, our understanding of transcriptomic ITH in OC, is still lacking. A recent study utilized the single-cell RNA sequencing approach to profile one single HGSOC tumour sample and identified two distinct cell populations. Both an epithelial cell populations and a separate population of mesenchymal, stem cell -like population were identified, reaffirming the prevalence of ITH in OC [24].

Ideally, a method that would comprehensively describe the co-existence of good and poor prognosis signatures [16] as well as drug-resistant and drug-sensitive populations [17] would better reflect the diversity that exist within a tumour lesion. Hence, we used a scheme termed molecular assessment of subtype heterogeneity (MASH) based on the established molecular subtypes previously described [6] to delineate the transcriptomic ITH in a cohort of 3,431 OC patients with associated clinical outcomes. MASH could be viewed as an extension to the single-subtype assignment method that also incorporates transcriptomic ITH to allow a more accurate prognostic view of a tumour. We also developed a clinically applicable NanoString-based assay that incorporates the MASH scheme.

Materials and Methods

National University Hospital cohort

From 2006 to 2014, frozen archival epithelial OC tumours, and cells from patient's ascites fluid from the Department of Obstetrics & Gynecology, National University of Singapore

were collected according to protocols approved by the Institution Review Board (supplementary material, Supplementary materials and methods). The samples were then subjected to microarray profiling using Affymetrix GeneChip® Human Gene 1.0 ST Array (Affymetrix, Inc., Santa Clara, CA) analysis (supplementary material, Supplementary materials and methods). The data has been deposited in Gene Expression Omnibus (GEO) with the accession id GSE94598. The data was first RMA-normalized and standardized with GSE69207 [27] using Affymetrix Power Tool version 1.15.0 and ComBat [45], respectively (supplementary material, Supplementary materials and methods). Subsequently, paired primary tumour-ascites data were extracted from the combined data.

Immunohistochemistry (IHC) analysis

Formalin-fixed and paraffin-embedded tissue sections (4 μm) from NUH cohort were immunostained for subtype-specific markers that were defined previously [6]: Epi-A-specific marker MUC16/CA-125 (1:50 dilution of Ov185.1; NeoMarker, Fremont, CA, USA), Mes marker α-SMA (1:1000 dilution of 1A4; Agilent (DAKO), Santa Clara, CA, USA), and Stem-A marker HMGA2 (1:50 dilution of OAGA00059, Aviva Systems Biology, San Diego, CA, USA.). Deparaffinization was performed using Histoclear and sections were rehydrated in a graded ethanol series. Antigen retrieval was performed by boiling at 120 °C in a high pH target retrieval solution for 10 minutes in a pressure cooker. Tissue sections were counterstained with haematoxylin, dehydrated in graded ethanols and mounted. All reagents for immunohistochemistry were from Agilent. The subtype-specific markers were validated using the positive controls (supplementary material, Figure S3).

Ovarian cancer database and subtype predictive model

OC molecular subtype information was extracted from CSIOVDB [27] curated from 48 cohorts of 3,431 clinical samples. Binary predictive models were developed to classify each subtype from the rest using Lasso regression and 10-fold cross-validation. The predicted subtype scores were scale-normalized across the samples to [0.0, 1.0], and a threshold of 0.4 was selected to call the presence of a subtype (supplementary material, Figure S1A). The procedure was repeated to derive subtype predictive model for OC cell lines.

Several datasets were downloaded from GEO and ArrayExpress for validation. Preprocessed data of E-MTAB-611 [35] were downloaded from ArrayExpress. Processed data from Australian Ovarian Cancer Study (AOCS) recurrent OC and ascites were downloaded from International Cancer Genome Consortium (ICGC; http://icgc.org/). Validation dataset GSE17260 [46], GSE32062 [47], and GSE32063 [47] hybridized on the Agilent platform, were downloaded from GEO, normalized using R version 3.3.1, limma version 3.28.21 and combined using ComBat [45] supplementary material, Supplementary materials and methods). The MASH analysis of these samples were estimated using the predictive model developed from CSIOVDB. Estimated tumour purity based on copy number and mutation data was extracted from [48] analysis of TCGA samples. Copy number aberration rate and tumour mutation rate were extracted from Broad GDAC data version 2016_01_28 [49].

Pathway and immune cell type infiltration

Selected microtubule and AXL pathways projections were computed using R version 3.3.1 Bioconductor package GSVA v1.20.0 [50], and genesets from the molecular signature database v5.1 [51]. Immune cell type infiltration was estimated using CIBERSORT [52].

Immune cell type markers were taken from NanoString Immune panel® annotation (https://www.nanostring.com).

Molecular subtype heterogeneity score

To estimate intra-tumoural heterogeneity, a quantitative measurement scheme was derived based on the scores computed by the five subtype predictors. This score is based on the assumption that a tumour must show at least one primary molecular subtype, and that the secondary subtypes constitute the intra-tumour molecular subtype heterogeneity. The rationale is based on reports that the co-existence of poor and good prognosis, chemo-sensitive and resistance signatures within a tumour [16,18]. Since the molecular subtypes in ovarian correlate to survival, this co-existence or mixture of good and poor prognosis cells would be indicative of heterogeneity which may be driven by various epigenomic or genomics aberration. Given the molecular subtype score $Score_s$, where $s \in$ **SUBTYPE**, and

$$\textbf{SUBTYPE} = \{\text{Epi-A, Epi-B, Mes, Stem-A, Stem-B}\}$$

, the tumour molecular subtype heterogeneity (MSH) score, denoted as $Tumor_{Heterogeneity}$, is estimated as

$$Tumor_{Heterogeneity} = \sum_{s \in \text{SUBTYPE}}^{5} Score_s - \max_{s \in \text{SUBTYPE}}(Score_s),$$

$$Tumor_{Heterogeneity} \in [-1.0, 4.0]$$

The MSH score was applied to the clinical samples. Tumours with more than one subtype annotation expectantly showed a higher heterogeneity score, indicating the validity of the scoring system (supplementary material, Figure S4A).

MASH assay

As the subtype signatures available on NanoString platform were derived previously from a cohort of 1,538 samples [6], new classifiers were developed for each subtype. For each

subtype classifier, the training were done on 49 or 61% of FFPE samples of NUH cohort, using lasso regression from Matlab 2016b, and MASH profile deducted from the CSIOVDB. The validation of the classifiers were assessed on the independent 31 or 39% of FFPE samples of NUH cohort. The cutoff for each subtype classifier is based on Youden's index that maximizes sensitivity and specificity on the ROC curve.

NanoString Codeset and processing

The 187 signature genes from a previous subtype analysis [6] were sent to NanoString (NanoString Technologies Inc; Seattle, WA, USA) for designing and customizing the nCounter CodeSets. FFPE samples from NUH cohort ($n = 80$) that had corresponding fresh frozen samples included in CSIOVDB were chosen and analysed using NanoString nCounter gene expression profiling. The normalization of NanoString data was performed using nSolver analysis software version 3.0 (NaonoString). The raw count from NanoString was subjected to background subtraction, positive control normalization and reference gene (*ACTB*, *B2M, GAPDH*, *HPRT1*, *HSP90*, *RPL90)* normalization. The normalized counts were then log2-transformed prior to down-stream analysis.

Statistical Analysis

Statistical analyses were conducted using Matlab® R2016b version 9.1.0.441655, and statistics and machine learning toolbox version 11.0 (MathWorks; Natick, MA, USA). Statistical significance of differential expression was evaluated using either Kruskal-Wallis (for paired comparison) or Mann-Whitney *U*-test. A Spearman correlation coefficient test was applied to assess significance of correlation. Kaplan-Meier analyses were conducted using GraphPad Prism® version 5.04 (GraphPad Software, La Jolla, CA, USA). Statistical significance of the Kaplan-Meier analysis was calculated by log-rank test. Pathway

enrichment scoring is based on Kolmogorov-Smirnov method described previously [31]. The Microtubule-related pathway geneset was taken from [6], and the AXL signalling signature from [53].

Conditional probability of subtype is estimated by counting the number of samples having subtype score > 0.4. Prior of each subtype is estimated by $P(subtype) = \frac{count_{subtype}}{N}$, where N is the total number of sample. The co-occurrence probability is computed by

$$P(subtype_{primary} AND\ subtype_{metastatsis}) = \frac{Count\ of\ Co-occurrence}{N}.$$

Conditional probability is subsequently computed by

$$P(subtype_{metastasis}|subtype_{primary})$$

$$= P(subtype_{primary} AND\ subtype_{metastasis}) \Big/ P(subtype_{primary})$$

For *de novo* clone formation, the conditional probability is computed by

$$P(subtype_{de\ novo\ metastasis}|subtype_{non-existence\ in\ primary})$$

$$= P(subtype_{de\ novo\ metastasis} AND\ subtype_{non-existense\ in\ primary}) \Big/ [1 - P(subtype_{primary})]$$

Results

Heterogeneity in ovarian cancer

OC is heterogeneous with 95% of ovarian tumours found to consist of at least four subclones [23]. Similarly, 82% of tumours from the ovarian cohort of TCGA [25] and 42% from the Mayo cohort [26] were also shown to consist of at least two molecular subtypes. To determine the extent of transcriptomic ITH that exists in OC, we explored the prevalence of multiple co-existent transcriptomic subtypes within ovarian tumours from a database of 3,431 OC samples—CSIOVDB [27]. We developed predictors for each transcriptomic subtype using Lasso regression (supplementary material, Figure S1; supplementary material, Supplementary materials ad methods) with an overall accuracy of 92.06% (supplementary material, Figure S1). Approximately 30% of tumours were found to consist of more than one subtype based on gene expression signatures (Figure 1B). Among various cohorts, tumours with more than one subtype ranged from 0 to 67% (supplementary material, Figure S2A). There was no significant association of tumour stage or grade with tumour heterogeneity (supplementary material, Figure S2B, C). When stratified according to histology, high grade endometrioid carcinomas were observed to be most heterogeneous followed by HGSOC (supplementary material, Figure S2D,E). There was no significant difference in tumour purity, copy number aberration rate, or mutation rate between tumours with single-subtype and tumours with more than one subtype (supplementary material, Figure S2F,G). We also found that there was no mutual exclusivity between which two molecular subtypes could co-exist within the same lesion (Figure 1C). Epi-B, the most prevalent transcriptomic subtype in OC, commonly co-existed with other subtypes (22.4%) (Figure 1C) while the Stem-B subtype, rarely co-existed with other subtypes (4.2%) (Figure 1C) partly because Stem-B largely consists of non-serous, low grade carcinoma which is commonly associated with tumours of low malignant potential [6]. Immunohistochemistry (IHC) analysis showed that

tumours with mixed molecular subtypes co-expressed markers and distinct patterns specific to each subtype (Figure 1D, supplementary material, Figure S3). In particular, Mes/Stem-A tumour showed high Mes marker α-SMA staining scattered within the tumour bulk region mixing with some infiltrating lymphocytes, with tumour cells showing strong nuclear staining of Stem-A marker HMGA2. Epi-B/Stem-A tumour showed solid sheets of cells with strong nuclear staining of Stem-A marker HMGA2 and relatively few infiltrating lymphocytes inside the tumour sheets and the stroma. Importantly, Mes marker α-SMA was confined to the periphery region without scattering within the tumour bulk. In contrast, in an Epi-B/Mes tumour, α-SMA staining not only was positive strongly at the infiltrating stroma but also moderately positive inside the cytoplasm of tumour cells. Numerous lymphocytes were seen trapped within the dense α-SMA stroma, suggesting an immune exclusion phenotype. The tumour cells were devoid of nuclear positivity for HMGA2. Intriguingly, both Epi-B subtype containing tumours showed absence of staining for the Epi-A marker MUC16/CA-125. Tumours of Epi-A/Mes mixture showed tumour cells with uniformly apical membrane staining for CA-125 and with α-SMA positive supporting stroma. The Mes/Stem-A tumours had patchy CA-125 positivity. Ovarian cancer is indeed enormously heterogeneous - manifested by displaying multiple molecular subtypes.

Heterogeneity in subtype composition impacts clinical outcomes.

An increased risk of recurrence or death has been associated with high ITH in several solid malignancies including lung [28], breast [29], head and neck cancers [30] and melanoma [29]. We evaluated whether high transcriptomic ITH would correlate with poorer outcomes in OC and developed a molecular subtype heterogeneity (MSH) score to estimate the degree of ITH within a tumour (Materials and methods). We observed that ovarian tumours had a wide range of MSH scores (supplementary material, Figure S4A). In general,

the MSH score was not significantly associated with DFS, OS or other clinicopathological parameters such as stage of disease, grade, surgical debulking status, age, clinical response, and EMT status (supplementary material, Figure S4B–D). However, when stratified by transcriptomic subtype, the degree of ITH was a pronounced aggravating factor in the good prognostic subtypes (Hazard Ratio = 1.2558; p-value = 0.0028) (Figure 2) as this negative impact on OS was particularly evident in Epi-A (HR = 4.4053; $p < 0.0001$) and Epi-B (HR = 1.3369; $p = 0.0174$) subtypes. In addition, multivariate Cox regression analyses with age, stage, grade, histology and debulking status further supported the role of the MSH score as an independent prognostic factor in Epi-A ($p = 0.0191$), with a trend to significance in Epi-B tumours ($p = 0.0792$; Table 1) for OS but not DFS. Upon further interrogation, we observed that the difference in survival outcomes between MSH low and high groups were attributed to the co-existence of poor prognostic subtypes (Mes or Stem-A) within the tumour composition (Figure 2).

We observed that the co-existence of Mes or Stem-A with other subtypes increased the EMT score of the tumour (Figure 3A) and was associated with a poorer prognosis. EMT score quantifies along a spectrum, which denotes the extent of mesenchymal traits that a tumour or cell line has acquired [31]. Tumours with Epi-A/Mes or Epi-A/Stem-A subtype had poorer OS and DFS compared to pure Epi-A tumours (HR = 1.6155, $p = 0.0752$, and HR = 1.8437, $p = 0.0211$, respectively; Figure 3B). A similar trend was observed when we compared Epi-B/Mes and Epi-B/Stem-A tumours to pure Epi-B tumours, albeit at a higher p value. When we interrogated the poor prognostic subtypes (Mes and Stem-A), the co-existence of both Mes/Stem-A subtypes within a tumour was observed to have the poorest OS, when compared to tumours consisting of pure Mes and Stem-A subtypes (HR = 1.583, $p = 0.0306$ and HR=1.91, $p = 0.0044$, respectively). Similarly, Mes/Stem-A tumours had a poorer DFS than pure Stem-A (HR = 2.089, $p = 0.0033$), and pure Mes tumours (HR = 1.405,

$p = 0.1221$), despite the non-significant difference in the later. The data suggest that ITH does contribute to poorer outcomes in OC with the molecular constituents within the tumour significantly influencing survival outcomes and the presence of poor prognostic subtype/s in a tumour significantly worsens clinical outcomes.

Since OC is characterized by frequent copy number aberration, we asked if MASH captures the genomic diversity within a tumour. We checked the copy number profiles of three genes which have been linked to molecular subtypes. *HMGA2* and *MYCN* copy number amplification was reported to be characteristic of Stem-A/C5 whereas *CCNE1* copy number amplification was linked to Epi-B/C2 tumours [32]. Samples with Stem-A containing subtypes, mixed or pure, had greater frequencies of *HMGA2* and *MYCN* amplifications compared to the non-Stem-A containing subtypes. Similarly, samples with Epi-B containing mixed or pure subtypes had more *CCNE1* amplification ($p < 0.0001$; supplementary material, Figure S5A). This indicates MASH still faithfully reflects the underlying genomic features within a tumour.

We applied MASH by using the subtype definition of CPTAC [10] (supplementary material, Supplementary materials and methods) on CSIOVDB. We observed that the OS of good prognosis subtype was worse when poor prognosis subtype co-existed within the tumour (supplementary material, Figure S5B), indicating the applicability of MASH could extend to other molecular subtyping scheme. Subsequently, we applied the MASH analysis on an independent cohort of 409 OC tumours (Materials and methods; supplementary material, Supplementary materials and methods) as a validation set, we observed the same trend with survival outcomes (supplementary material, Figure S5C). Because of the small sample size and limited number of events, the difference in outcomes in this validation cohort between the Mes/Stem-A and pure Mes or Stem-A tumours were not significant ($p = 0.476$, and $p = 0.172$). Yet, the combination of Mes/Stem-A still appeared to confer a worse

outcome than Mes or Stem-A alone, as indicated by the hazard ratio HR = 1.5669, and HR = 2.7064, respectively. There were insufficient samples for comparisons between Epi-A with Epi-A mixtures ($n = 4$; supplementary material, Figure S5C), and hence a survival analysis was not performed. In comparison of Epi-B/Mes or Epi-B/Stem-A and Epi-B tumours of the validation cohort, the trend was concordant with the above mentioned CSIOVDB cohort where significant poorer OS was observed but not in DFS (HR = 6.6401, $p < 0.0001$; and HR = 1.1744, $p = 0.4964$, respectively; supplementary material, Figure S5C). In the validation cohort, Epi-B/Mes and Epi-B/Stem-A tumours were combined due to the low number of samples available.

Clinical outcome is linked to the extent of poor prognostic subtype within a tumour

Armed with the knowledge that the co-existence of Mes and Stem-A subtypes conferred the worst outcome, we explored whether the degree of Mes/Stem-A mixture would also impact patient outcomes. We analysed the percentages of Mes/Stem-A mixture within a tumour, using the MASH scheme, and correlated them with clinical outcomes (Figure 3C). We grouped the tumours into three nominal categories according to the degree of Mes/Stem-A mixture: none – no Mes/Stem-A subclones within a tumour; partial – Mes/Stem-A subclones make up 1~99% of tumour; or complete – tumour consist of only Mes/Stem-A subtype clones. Consistently, we found that the higher percentage of Mes/Stem-A subtype present within a tumour significantly correlated with OS and DFS in the CSIOVDB cohort (Figure 3C, supplementary material, Figure S6A; $p < 0.0001$). OC patients without Mes/Stem-A subtype clones had 19 months longer median overall survival compared to those with tumours completely consisting of Mes/Stem-A clones (55 versus 36 months in OS, and 24 versus 16 months in DFS, respectively). We observed highly similar OS and DFS trends

in the validation cohort ($p = 0.0212$ and 0.0048, respectively) as well as in the International Cancer Genome Consortium-Australian Ovarian Cancer Study (ICGC-AOCS) chemoresistant OC cohort (release 19) [3] ($p = 0.0473$ and 0.4371, respectively). Patients with low Mes/Stem-A trait were observed to have a 23 months longer median survival than those with high Mes/Stem-A trait (44 versus 21 months in OS, and 7 versus 4 months in DFS, respectively). It is worth noting that slightly different stratification methods were used in the CSIOVDB and ICGC-AOCS cohorts because of the inherent differences between the analyses of tumour samples from the two cohorts (RNA-seq versus microarray) (supplementary material, Supplementary materials and methods).

Enrichment of Mes and Stem-A subtypes in recurrent and metastatic OC

We evaluated the evolution of the transcriptomic subtypes through the course of disease from diagnosis to disease relapse. We applied the MASH scheme to paired tumour samples comparing primary tumour with metastatic/recurrent disease including ascitic cells from the same patient. Intriguingly, regardless of the initial subtype of the primary ovarian tumour sample, the subsequent omental metastasis GSE30587 [33], peritoneum metastasis FRTLO [34], and/or ascitic cells of patients (GSE94598) at recurrent disease, consistently showed an increase in the percentage of Mes or Stem-A subtype (Figure 4A). The same trend of Mes or Stem-A enrichment was also seen in platinum-resistant relapsed disease compared to the primary tumours in two separate independent cohorts E-MTAB-611 [35], and ICGC-AOCS [3] (supplementary material, Supplementary materials and mrthods). When paired primary-metastatic tumours were analysed, there was significant enrichment of Mes/Stem-A in the metastatic deposits compared to primary tumours ($p = 0.0063$; Figure 4B; supplementary material, Figure S6B). We subsequently explored whether the poor prognostic subtypes influenced response to chemotherapy. We observed no significant enrichment of

Mes/Stem-A in tumours that did not respond to chemotherapy ($p = 0.9468$; supplementary material, Figure S6C).

Comparing paired primary and metastatic or relapsed tumour samples (Materials and Methods), we found the majority of metastatic or relapsed tumour samples were more likely to fall into the Mes subtype regardless of the primary tumour subtype (Figure 4C). The Epi-A subtype had a higher tendency to maintain the original subtype or to switch to the Mes subtype at relapse or during metastasis while the Stem-A subtype appeared to have an affinity for switching only to Mes subtype (Figure 4C). The Mes subtype was observed to be stable maintaining the transcriptomic signature in disease relapse and during metastasis (Figure 4C). To further understand the evolutionary changes in the subtypes from primary to recurrent/metastatic disease, we used MASH to delineate the constituents of primary and recurrent tumours and subsequently divided them into three different categories: (i) clonal conversion - the disappearance of a subtype clone initially observed in primary tumour from the metastatic lesion, (ii) clonal expansion - expansion of a pre-existing subtype clone within the primary in the metastatic deposit, or (iii) *de novo* − the appearance of a subtype in the metastatic deposit which was not originally seen in the primary tumour (Figure 4C). The Mes subtype had the highest probability to undergo clonal expansion and to appear in metastasis or chemoresistant relapse. In contrast, the Stem-A and Epi-B subtypes were more likely to undergo clonal conversion to other subtypes. For the Stem-A subtype, it was very unlikely to acquire this subtype during disease progression unless there was a pre-existing Stem-A clone in the primary tumour (Figure 4C). This likely reflects the stem cell-like nature of the Stem-A subtype. We also observed that almost all subtypes (except Stem-A) showed medium probability to be annotated as Epi-B in the metastatic lesion. In accordance, Epi-B also had the second highest probability to form *de novo* clones in metastatic lesions. Since Epi-B is correlated with the immune reactive subtype from TCGA, this finding is intriguing and raises

the question regarding the impact of local microenvironmental cues in ITH and disease progression. It also shines light on the relationship between the microenvironment and the immune signature in its effect on biological function and even therapeutic responses. Accordingly, we checked the immune cell infiltration and immune cell type markers for tumours that underwent clonal expansion of Epi-B and Mes. There was a change in immune environment from primary to recurrent/metastasis settings (supplementary material, Figure S6D,E). Tumours that underwent Epi-B clonal expansion showed increased infiltration of resting memory CD4 T-cells (supplementary material, Figure S6D). On the other hand, tumours that underwent clonal expansion of Mes had increased infiltration of monocytes and tumour-associated macrophages M2 (supplementary material, Figure S6E), which is consistent with the roles of monocytes and macrophages in promoting tumour growth [36]. However, these observations on clonal conversion and *de novo* clone formation should be accepted with caution. The probability of clonal expansion may be underestimated in our analysis due to the lack of multiple biopsies taken from the primary and metastatic tumour samples to confirm the presence of spatially separated existing subclones. Collectively, these results indicate that during OC progression, transcriptomic subtype clones undergo clonal evolution according to several distinct patterns as a result of either clonal expansion, clonal conversion, or *de novo* clone formation leading to significant intra- and inter-tumoural heterogeneity observed between paired samples of primary tumour and metastatic/ relapsed lesions.

Utility of MASH as a clinical assay

As the significance of molecular subtyping in OC becomes more apparent, clinical trials using molecular signatures as a biomarker to stratify patients for specific therapeutic strategies are now underway (clinicaltrials.gov identifier: NCT03188159). Applying MASH, we observed that the underlying subtype mixture critically affects the targeted pathway

activity (supplementary material, Supplementary materials and methods, and Figure S7), which may alter the therapeutic response of a tumour. Therefore, it is perhaps intuitive to incorporate transcriptomic heterogeneity into a clinically applicable assay for better stratification of these patients. Using fresh frozen and FFPE samples collected from 80 OC patients from 2006 to 2014, we applied the MASH analysis using microarray and NanoString gene expression profiling methods (Figure 5A). In the fresh frozen samples subjected to microarray analysis, 61.25% ($n = 49$) were assigned a single-subtype while 38.75% ($n = 31$) were mixed-subtypes (Table 2) based on the MASH scheme. The most frequent subtype mixture was Epi-B/Stem-A ($n = 9$; 11.3%) followed by Epi-B/Stem-B ($n = 8$; 10%) and Epi-B/Epi-A ($n = 6$; 7.5%). We took the MASH profiles obtained from microarray as supervised training labels to develop a MASH classifier for the NanoString assay. FFPE samples from patients assigned to a single subtype ($n = 49$) were used to train the NanoString MASH classifier (Figure 5B; Material and methods). The remaining FFPE samples ($n = 31$) not used in NanoString MASH classifier training were subsequently annotated based on the predicted enrichment scores of the 5 molecular subtypes. The prediction was compared with the MASH analysis using the microarray method (Figure 5B). The NanoString MASH assay achieved an average area under the curve (AUC) of 0.971 for training, and 0.757 for testing sets, showing good feasibility of this assay. Of note, the Mes and Stem-A classifiers had AUCs of 0.705 and 0.86, respectively. Receiver-operating characteristic (ROC) curves for each subtype showed good accuracy of the classifier based on the testing cohort, apart from Epi-B (Figure 5C). The poor performance of Epi-B is due to limited numbers of non-Epi-B samples in the testing set ($n = 3$), which significantly deflates the specificity for each wrongly classified sample. Encouragingly, the propensity to accurately detect the poor prognostic subtypes Mes or Stem-A within the MASH, was 85.7% (training set) and 67.8% (testing set; supplementary material, Table S1). Importantly, the age of FFPE tumour samples did not impact on the

results as the majority of the FFPE samples were at least 3 years old, with some noted to be >10 years old. Collectively, these results demonstrate the feasibility of accurately implementing the MASH scheme as a clinical assay using easily obtained FFPE samples.

Discussion

As we enter the era of precision medicine, managing the underlying heterogeneity within tumours continues to be one of the most challenging tasks. Many studies have looked at the mutational landscape using next-generation sequencing (NGS) which have helped shine some light in this field. With sequencing tools available at the single-cell level, the appreciation of the dynamic intricacies of inter- and intra-tumour heterogeneity (ITH) has been greatly magnified. Yet, there are limitations before these technologies can be readily translated into the clinical setting and be offered as diagnostic tests. In this study, we demonstrated that MASH captures the ITH from the bulk tumour gene expression profiling and provide additional clinically relevant information, a strength over the conventional single-subtype assignment. Indeed, when Chen, *et al* [37] attempted to re-implement three previously validated subtyping methods [7,25,32], they observed only a minority of HGSOC fell into the four subtypes while a majority of samples (~75%) were not consistently labelled into the pre-specified single subtypes. This is likely due to the analysed tumours being mixed consisting of several transcriptomic subtypes and were unable to fit neatly into a single assigned subtype, highlighting the heterogeneous nature of ovarian tumours that often display more than 1 molecular subtype, as demonstrated in our study. Hence, we proposed a scheme termed—molecular assessment of subtype heterogeneity (MASH)—to describe a tumour using its molecular subtype composition.

The MASH scheme also provides a cheaper alternative to single-cell/nucleus technologies. While useful to quantify and study ITH, single-cell/nucleus technologies may not be cost-effective and can be technically burdensome for use in clinical practice. We demonstrated that MASH can feasibly be applied to NanoString® gene expression profiling technology using readily available FFPE samples, to facilitate translation into clinical practice in a cost-effective manner. In addition, the MASH annotation using the bulk tumour

transcriptome could circumvent a crucial technical issue encountered in single-cell/nucleus analysis: how many single cells are required to accurately represent the lesion in question? Nonetheless, this study is still limited by the fact that the archival samples were derived from a single random biopsy. The extensive diversity in tumours poses significant challenges in resolving the full spectrum of cancer pathway aberrations through a single biopsy sampling bias and may not be representative of the entire tumour [16]. Consequently, this raises concerns whether the subtype annotation derived from a single biopsy would adequately depict the degree of genetically distinct subclones driving phenotypic variation of the actual tumour. However, the above concerns could be somewhat reduced by the temporal evolution of the poor prognostic signatures demonstrated in this study, where the presence of poor prognostic subtypes within a tumour persisted in the recurrence/metastatic setting and ultimately determined the patients clinical outcome. As the Mes signature is enriched in processes related to extracellular matrix modelling, stroma and fibroblast [3], it is entirely plausible that OC preferentially elicits stromal reactions similar to fibrosis in response to platinum-taxane chemotherapy. It is also plausible that the tumour stromal and immune environment were remodelled in the recurrent setting in favour of tumour progression.

The co-existence of multiple molecular subtypes or subclones within a tumour implies that more sophisticated therapeutic strategies are required in order to successfully target all the specific subtypes/subclones [39,40]. Treatment regimens targeting only one subtype might inevitably spare the other co-existing subtypes resulting in the expansion of or conversion to more resistant clones [21,22,40]. In our study, we identified Mes and Stem-A subtypes predominated in the recurrence or metastatic setting suggesting targeting of unique aberrant pathways responsible for driving the individual poor prognostic subtypes should be explored. We also demonstrated that the Mes subtype is least likely to undergo clonal conversion suggesting poor prognostic outcomes in patients with even a small percentage of

Mes subtype in their original primary tumour and a combination approach that targets the different clones within a tumour is likely required [41].

An important point of contention is the extent of subclones presents that would be considered relevant for therapeutic targeting. This is an important consideration highlighted in the KEYNOTE-010 study where consistent benefit of PD-L1 inhibition by pembrolizumab was only demonstrated in non-small cell lung cancer patients with $\geq 50\%$ of PD-L1 expression in tumours, but ambiguous for patients with PD-L1 expression $< 50\%$ [42]. The challenge is how to set the cut-off for a given biomarker (MASH in this case) that would have the highest impact for therapeutic response. An important aspect not covered in our study was inter-subclone cooperation [43]. Co-existing molecular subtypes within a tumour might interact and cooperate or compete in response to microenvironmental cues and cytotoxic stress. While it may be plausible to use the MASH scheme to analyse such interaction, the results will at best be correlative and therefore, limited in value. In this regard, single-cell transcriptome analysis is the preferred method when evaluating inter-subclone competition and cooperation functionally.

Applying various molecular subtype definitions from Tothill, *et al*, TCGA, or CPTAC would likely yield similar results with good overlap [6,10]. Since transcriptomic quantification technologies are relatively consistent especially in quantifying highly expressed transcripts [44], MASH could be applicable to any transcript quantification platform of choice. Nonetheless, our study shows that the application of the MASH scheme in deciphering ITH offers a promising method as a clinical tool. Thus, the proposed MASH scheme may provide a promising strategy in informing personalized management of a patient.

Author contribution statement

R.Y.H, T.Z.T, D.S.P.T., J.L, and M.C designed and conceptualised the study. J.Y performed sample collection and experiments. D.L processed and reviewed samples and FFPE. T.Z.T. performed bioinformatics analysis. R.Y.H, T.Z.T, V.H., D.S.P.T., J.L, M.C, and C.S. analysed the data, interpret the results, and wrote the manuscript.

References

1.   Torre LA, Bray F, Siegel RL, *et al.* Global cancer statistics, 2012. *CA Cancer J Clin* 2015; **65:** 87–108.

2.   Alsop K, Fereday S, Meldrum C, *et al.* BRCA mutation frequency and patterns of treatment response in BRCA mutation-positive women with ovarian cancer: a report from the Australian Ovarian Cancer Study Group. *J Clin Oncol* 2012; **30:** 2654–2663.

3.   Patch AM, Christie EL, Etemadmoghadam D, *et al.* Whole-genome characterization of chemoresistant ovarian cancer. *Nature* 2015; **521:** 489–494.

4.   Etemadmoghadam D, George J, Cowin PA, *et al.* Amplicon-dependent CCNE1 expression is critical for clonogenic survival after cisplatin treatment and is correlated with 20q11 gain in ovarian cancer. *PLoS One* 2010; **5:** e15498.

5.   Tan DS, Rothermundt C, Thomas K, *et al.* "BRCAness" syndrome in ovarian cancer: a case-control study describing the clinical features and outcome of patients with epithelial ovarian cancer associated with BRCA1 and BRCA2 mutations. *J Clin Oncol* 2008; **26:** 5530–5536.

6.   Tan TZ, Miow QH, Huang RY, *et al.* Functional genomics identifies five distinct molecular subtypes with clinical relevance and pathways for growth control in epithelial ovarian cancer. *EMBO Mol Med* 2013; **5:** 983–998.

7.   Tothill RW, Tinker AV, George J, *et al.* Novel molecular subtypes of serous and endometrioid ovarian cancer linked to clinical outcome. *Clin Cancer Res* 2008; **14:** 5198–5208.

8.   Burrell RA, McGranahan N, Bartek J, *et al.* The causes and consequences of genetic heterogeneity in cancer evolution. *Nature* 2013; **501:** 338–345.

9.   Cancer Genome Atlas Research N. Integrated genomic analyses of ovarian carcinoma. *Nature* 2011; **474:** 609–615.

10.   Zhang H, Liu T, Zhang Z, *et al.* Integrated proteogenomic characterization of human high-grade serous ovarian cancer. *Cell* 2016; **166:** 755–765.

11.   Gourley C, McCavigan A, Perren T, *et al.* Molecular subgroup of high-grade serous ovarian cancer (HGSOC) as a predictor of outcome following bevacizumab. *J Clin Oncol* 2014; **32:** No. 15_suppl 5502.

12.   Kommoss S, Winterhoff B, Oberg A, *et al.* Bevacizumab may differentially improve ovarian cancer outcome in patients with proliferative and mesenchymal molecular subtypes. *Clin Cancer Res* 2017; **23:** 3794–3801.

13.   George J, Alsop K, Etemadmoghadam D, *et al.* Nonequivalent gene expression and copy number alterations in high-grade serous ovarian cancers with BRCA1 and BRCA2 mutations. *Clin Cancer Res* 2013; **19:** 3474–3484.

14.   Miow QH, Tan TZ, Ye J, *et al.* Epithelial-mesenchymal status renders differential responses to cisplatin in ovarian cancer. *Oncogene* 2015; **34:** 1899–1907.

15.   Zardavas D, Irrthum A, Swanton C, *et al.* Clinical management of breast cancer heterogeneity. *Nat Rev Clin Oncol* 2015; **12:** 381–394.

16.   Gerlinger M, Rowan AJ, Horswell S, *et al.* Intratumor heterogeneity and branched evolution revealed by multiregion sequencing. *N Engl J Med* 2012; **366:** 883–892.

17.   Kim KT, Lee HW, Lee HO, *et al.* Single-cell mRNA sequencing identifies subclonal heterogeneity in anti-cancer drug responses of lung adenocarcinoma cells. *Genome Biol* 2015; **16:** 127.

18.   Brocks D, Assenov Y, Minner S, *et al.* Intratumor DNA methylation heterogeneity reflects clonal evolution in aggressive prostate cancer. *Cell Rep* 2014; **8:** 798–806.

19.   McPherson A, Roth A, Laks E, *et al.* Divergent modes of clonal spread and intraperitoneal mixing in high-grade serous ovarian cancer. *Nat Genet* 2016; **48:** 758–767.

20.   Reardon DA, Wen PY. Glioma in 2014: unravelling tumour heterogeneity-implications for therapy. *Nat Rev Clin Oncol* 2015; **12:** 69–70.

21.   Kemper K, Krijgsman O, Cornelissen-Steijger P, *et al.* Intra- and inter-tumor heterogeneity in a vemurafenib-resistant melanoma patient and derived xenografts. *EMBO Mol Med* 2015; **7:** 1104–1118.

22. Landau DA, Carter SL, Stojanov P*, et al.* Evolution and impact of subclonal mutations in chronic lymphocytic leukemia. *Cell* 2013; **152:** 714–726.

23. Lohr JG, Stojanov P, Carter SL*, et al.* Widespread genetic heterogeneity in multiple myeloma: implications for targeted therapy. *Cancer Cell* 2014; **25:** 91–101.

24. Winterhoff BJ, Maile M, Mitra AK*, et al.* Single cell sequencing reveals heterogeneity within ovarian cancer epithelium and cancer associated stromal cells. *Gynecol Oncol* 2017; **144:** 598–606.

25. Verhaak RG, Tamayo P, Yang JY*, et al.* Prognostically relevant gene signatures of high-grade serous ovarian carcinoma. *J Clin Invest* 2013; **123:** 517–525.

26. Konecny GE, Wang C, Hamidi H*, et al.* Prognostic and therapeutic relevance of molecular subtypes in high-grade serous ovarian cancer. *J Natl Cancer Inst* 2014; **106**.

27. Tan TZ, Yang H, Ye J*, et al.* CSIOVDB: a microarray gene expression database of epithelial ovarian cancer subtype. *Oncotarget* 2015; **6:** 43843–43852.

28. Jamal-Hanjani M, Wilson GA, McGranahan N*, et al.* Tracking the evolution of non-small-cell lung cancer. *N Engl J Med* 2017; **376:** 2109–2121.

29. Morris LG, Riaz N, Desrichard A*, et al.* Pan-cancer analysis of intratumor heterogeneity as a prognostic determinant of survival. *Oncotarget* 2016; **7:** 10051–10063.

30. Mroz EA, Tward AD, Hammon RJ*, et al.* Intra-tumor genetic heterogeneity and mortality in head and neck cancer: analysis of data from the Cancer Genome Atlas. *PLoS Med* 2015; **12:** e1001786.

31. Tan TZ, Miow QH, Miki Y*, et al.* Epithelial-mesenchymal transition spectrum quantification and its efficacy in deciphering survival and drug responses of cancer patients. *EMBO Mol Med* 2014; **6:** 1279–1293.

32. Helland A, Anglesio MS, George J*, et al.* Deregulation of MYCN, LIN28B and LET7 in a molecular subtype of aggressive high-grade serous ovarian cancers. *PLoS One* 2011; **6:** e18064.

33. Brodsky AS, Fischer A, Miller DH*, et al.* Expression profiling of primary and metastatic ovarian tumors reveals differences indicative of aggressive disease. *PLoS One* 2014; **9:** e94476.

34. Malek JA, Martinez A, Mery E*, et al.* Gene expression analysis of matched ovarian primary tumors and peritoneal metastasis. *J Transl Med* 2012; **10:** 121.

35. Marchini S, Fruscio R, Clivio L*, et al.* Resistance to platinum-based chemotherapy is associated with epithelial to mesenchymal transition in epithelial ovarian cancer. *Eur J Cancer* 2013; **49:** 520–530.

36. Chittezhath M, Dhillon MK, Lim JY*, et al.* Molecular profiling reveals a tumor-promoting phenotype of monocytes and macrophages in human cancer progression. *Immunity* 2014; **41:** 815–829.

37. Chen GM, Kannan L, Geistlinger L*, et al.* Consensus on molecular subtypes of high-grade serous ovarian carcinoma. *Clin Cancer Res* 2018; **24:** 5037–5047.

38. Chen GM, Kannan L, Geistlinger L*, et al.* Consensus on molecular subtypes of ovarian cancer. *bioRxiv* 2017**:** 162685.

39. Prat A, Bianchini G, Thomas M*, et al.* Research-based PAM50 subtype predictor identifies higher responses and improved survival outcomes in HER2-positive breast cancer in the NOAH study. *Clin Cancer Res* 2014; **20:** 511–521.

40. McGranahan N, Swanton C. Biological and therapeutic impact of intratumor heterogeneity in cancer evolution. *Cancer Cell* 2015; **27:** 15–26.

41. Willyard C. Cancer therapy: an evolved approach. *Nature* 2016; **532:** 166–168.

42. Herbst RS, Baas P, Kim DW*, et al.* Pembrolizumab versus docetaxel for previously treated, PD-L1-positive, advanced non-small-cell lung cancer (KEYNOTE-010): a randomised controlled trial. *Lancet* 2016; **387:** 1540–1550.

43. Cleary AS, Leonard TL, Gestl SA*, et al.* Tumour cell heterogeneity maintained by cooperating subclones in Wnt-driven mammary cancers. *Nature* 2014; **508:** 113–117.

44. Zhang W, Yu Y, Hertwig F*, et al.* Comparison of RNA-seq and microarray-based models for clinical endpoint prediction. *Genome Biol* 2015; **16:** 133.

45. Johnson WE, Li C, Rabinovic A. Adjusting batch effects in microarray expression data using empirical Bayes methods. *Biostatistics* 2007; **8:** 118–127.

46. Yoshihara K, Tajima A, Yahata T*, et al.* Gene expression profile for predicting survival in advanced-stage serous ovarian cancer across two independent datasets. *PLoS One* 2010; **5:** e9615.

47. Yoshihara K, Tsunoda T, Shigemizu D*, et al.* High-risk ovarian cancer based on 126-gene expression signature is uniquely characterized by downregulation of antigen presentation pathway. *Clin Cancer Res* 2012; **18:** 1374–1385.

48. Aran D, Sirota M, Butte AJ. Systematic pan-cancer analysis of tumour purity. *Nat Commun* 2015; **6:** 8971.

49. Broad Institute TCGA GDAC. Firehose stddata_2016_01_28 run. Broad Institute of MIT and Harvard, 2016 [http://gdac.broadinstitute.org/runs/info/DOIs__stddata.html].

50. Hanzelmann S, Castelo R, Guinney J. GSVA: gene set variation analysis for microarray and RNA-seq data. *BMC Bioinformatics* 2013; **14:** 7.

51. Subramanian A, Tamayo P, Mootha VK*, et al.* Gene set enrichment analysis: a knowledge-based approach for interpreting genome-wide expression profiles. *Proc Natl Acad Sci U S A* 2005; **102:** 15545–15550.

52. Newman AM, Liu CL, Green MR*, et al.* Robust enumeration of cell subsets from tissue expression profiles. *Nat Methods* 2015; **12:** 453–457.

53. Antony J, Tan TZ, Kelly Z*, et al.* The GAS6-AXL signaling network is a mesenchymal (Mes) molecular subtype-specific therapeutic target for ovarian cancer. *Sci Signal* 2016; **9:** ra97.

Tables

Table 1A. Univariate and Multivariate Cox regression analyses of overall survival.

Single Subtype Samples $n = 711$, event = 345		Sample Number	Univariate			Multivariate		
Parameter	**Category**		**Coefficient**	**Hazard^**	**p-value**	**Coefficient**	**Hazard^**	**p-value**
Age	<55	225	0.3326	1.395 (1.097-1.772)	0.0065	0.2881	1.334 (1.0491-1.696)	0.0187
	≥ 55	486						
Stage	I, II	69	1.425	4.157 (2.143-8.062)	2.5E-5	1.0844	2.958 (1.5078-5.801)	0.0016
	III, IV	642						
Grade	G1	28	1.3327	3.791 (1.566-9.181)	0.0031	0.8705	2.388 (0.9784-5.829)	0.0559
	G2, G3	683						
Debulk Status	Optimal	485	0.2939	1.342 (1.08-1.667)	0.0079	0.1394	1.15 (0.923-1.432)	0.2133
	Suboptimal	226						
Histology	Non-high grade serous	37	1.654	5.23 (1.678-16.3)	0.0044	1.1439	3.139 (0.9989-9.864)	0.0502
	High grade serous	674						
Molecular Subtype Heterogeneity Score	< median	355	0.2193	1.245 (1.007-1.54)	0.0429	0.1255	1.134 (0.9158-1.404)	0.2492
	≥ median	356						

^ 95% confidence interval in parentheses

Stratified by Subtype		Epi-A $n = 56$, event = 22			Epi-B $n = 292$, event = 133			Stem-B $n = 23$, event = 6			Mes $n = 200$, event = 108			Stem-A $n = 140$, event = 77		
Parameter	**Category**	#	Coef.	*p*	#	Coef.	*p*	#	Coef.	*p*	#	Coef.	*p*	#	Coef.	*p*
Age	<55	22	0.4709	0.3766	101	0.1663	0.3757	10	0.9183	0.433	62	0.281	0.221	30	0.5145	0.0949
	≥ 55	34			191			13			138			110		
Stage	I, II	14	17.02	0.9985	32	1.6418	0.0126	7	0.657	0.657	6	16.78	0.994	10	-0.5145	0.2727
	III, IV	42			260			16			194			130		
Grade	G1	17	0.2893	0.6833	2	-1.0062	0.3873	3	18.85	0.999	5	0.4198	0.678	1	17.09	0.9999
	G2, G3	39			290			20			195			139		
Debulk Status	Optimal	48	1.12	0.0526	201	0.1735	0.3312	20	0.7862	0.479	115	0.08425	0.672	101	-0.0968	0.6996
	Suboptimal	8			91			3			85			39		
Histology	Non-high grade serous	16	17.25	0.9984	7	0.5969	0.5717	7	-0.1125	0.926	4	0.7412	0.467	3	17.46	0.9964
	High grade serous	40			285			16			196			137		

| MSH Score | < median | 28 | 1.499 | 0.0191 | 146 | 0.3114 | 0.0792 | 11 | -0.323 | 0.805 | 100 | - | 0.791 | 70 | - | 0.60 |
| | ≥ median | 28 | | | 146 | | | 12 | | | 100 | 0.0523 | | 70 | 0.1197 | 63 |

Abbrev: #, sample number; Coef., multivariate Cox's regression coefficient; MSH, molecular subtype heterogeneity.

Table 1B. Univariate and Multivariate Cox regression analyses of disease-free survival.

Single Subtype Samples		Sample Number	Univariate			Multivariate		
n = 560, event = 380								
Parameter	**Category**		**Coefficient**	**Hazard^**	***p*-value**	**Coefficient**	**Hazard^**	***p*-value**
Age	<55	186	0.3072	1.36 (1.091-1.694)	0.00622	0.2277	1.25560 (1.00620-1.56700)	0.04391
	≥ 55	374						
Stage	I, II	59	1.6074	4.99 (3.018-8.248)	3.65E-10	1.3049	3.68740 (2.20540-6.16500)	6.5E-07
	III, IV	501						
Grade	G1	18	1.2302	3.422 (1.617-7.244)	0.0013	0.4523	1.57200 (0.73010-3.38500)	0.24768
	G2, G3	542						
Debulk Status	Optimal	403	0.5018	1.652 (1.336-2.042)	3.6E-06	0.2933	1.34080 (1.08200-1.66200)	0.00736
	Suboptimal	157						
Histology	Non-high grade serous	30	1.603	4.967 (2.462-10.02)	7.58E-06	1.0718	2.9207 (1.4262-5.981)	0.00338
	High grade serous	530						
Molecular Subtype Heterogeneity Score	< median	273	0.03759	1.038 (0.8481-1.271)	0.716	-0.1094	0.8964 (0.7311-1.099)	0.29288
	≥ median	287						

^ 95% confidence interval in parentheses

Stratified by Subtype		Epi-A			Epi-B			Stem-B			Mes			Stem-A		
		n = 47, event = 21			*n* = 235, event = 163			*n* = 19, event = 7			*n* = 158, event = 119			*n* = 106, event = 70		
Parameter	**Category**	#	Coef.	*p*	#	Coef.	*p*	#	Coef.	*p*	#	Coef.	*p*	#	Coef.	*p*
Age	<55	17	0.7355	0.2159	87	0.1442	0.3915	9	0.3436	0.8138	50	0.1769	0.391	28	0.5176	0.0941
	≥ 55	30			148			10			108			78		
Stage	I, II	14	19.71	0.9983	32	1.4022	1.79E-05	4	21.32	0.999	5	16.86	0.993	9	0.5762	0.2731
	III, IV	33			203			15			153			97		
Grade	G1	14	-0.3076	0.691	2	-1.4803	0.0719	3	19.25	0.9986	4	-0.155	0.831	0	NA	NA
	G2, G3	33			233			16			154			106		
Debulk Status	Optimal	40	0.963	0.0832	177	0.1597	0.3661	16	2.56	0.0418	98	0.1273	0.512	77	0.414	0.1152
	Suboptimal	7			58			3			60			29		
Histolog	Non-high grade serous	16	19.56	0.998	6	0.265	0.6512	7	-1.683	0.193	4	1.44	0.172	2	0.379	0.73

		#	Coef.		#	Coef.		#	Coef.		#	Coef.		#	Coef.	
y	High grade serous	31		3	229	1		12		3	154			104	1	87
MSH Score	< median	23	0.774	0.261	117	-	0.1583	9	-1.084	0.350	79	-0.303	0.109	53	0.303	0.22
	≥ median	24	4	4	118	0.227 7		10		7	79			53	1	95

Abbrev: #, sample number; Coef., multivariate Cox's regression coefficient; NA, not applicable; MSH, molecular subtype heterogeneity

Table 2. NUH cohort for NanoString assay development

Co-occurrence frequency	Epi-A	Epi-B	Stem-B	Mes	Stem-A	Total
Epi-A	5 (6.3%)					
Epi-B	6 (7.5%)	11 (13.8%)				
Stem-B	1 (1.3%)	8 (10%)	10 (12.5%)			
Mes	1 (1.3%)	5 (6.3%)	0 (0%)	14 (17.5%)		
Stem-A	0 (0%)	9 (11.3%)	0 (0%)	1 (1.3%)	9 (11.3%)	
Single-subtype	5 (6.3%)	11 (13.8%)	10 (12.5%)	14 (17.5%)	9 (11.3%)	49 (61.25%)
Mixed-subtype	8 (10%)	22 (27.5%)	0 (0.0%)	1 (1.3%)	0 (0%)	39 (38.75%)

Figure Legends

**Figure 1. Ovarian cancer is extremely heterogeneous between tumours and within tumours.**

(A) Epithelial ovarian cancer can be classified into five molecular subtypes: good prognosis (Epi)thelial-A/C3/Differentiated, (Epi)thelial-B/C4/Immunoreactive, (Stem)-like-B/C6; and poor prognosis (Mes)enchymal/C1/Mesenchymal, (Stem)-like-A/C5/Proliferative. Labels are given in order of Tan, *et al* [6]/Tothill, *et al* [7]/TCGA [9].

(B) Pie chart of CSIOVDB samples exhibiting multiple subtypes. The threshold of normalized subtype score 0.4 was deemed if a subtype properties are expressed. Colour code: 1 subtype, black; 2 subtype, red; 3 subtype, pink.

(C) Chart of subtype co-occurrence frequency in CSIOVDB samples. Frequency percentage is given in parentheses.

(D) Immunohistochemistry staining for subtypes markers (Epi-A, MUC16/CA-125; Mes, α-SMA; Stem-A, HMGA2) in ovarian cancer with mixed subtypes. Scale bars = 100 μm. *indicates α-SMA on a separate tumour region of patient 1-1309.

The frequency percentages in B, C are computed based on CSIOVDB sample size of 3,431.
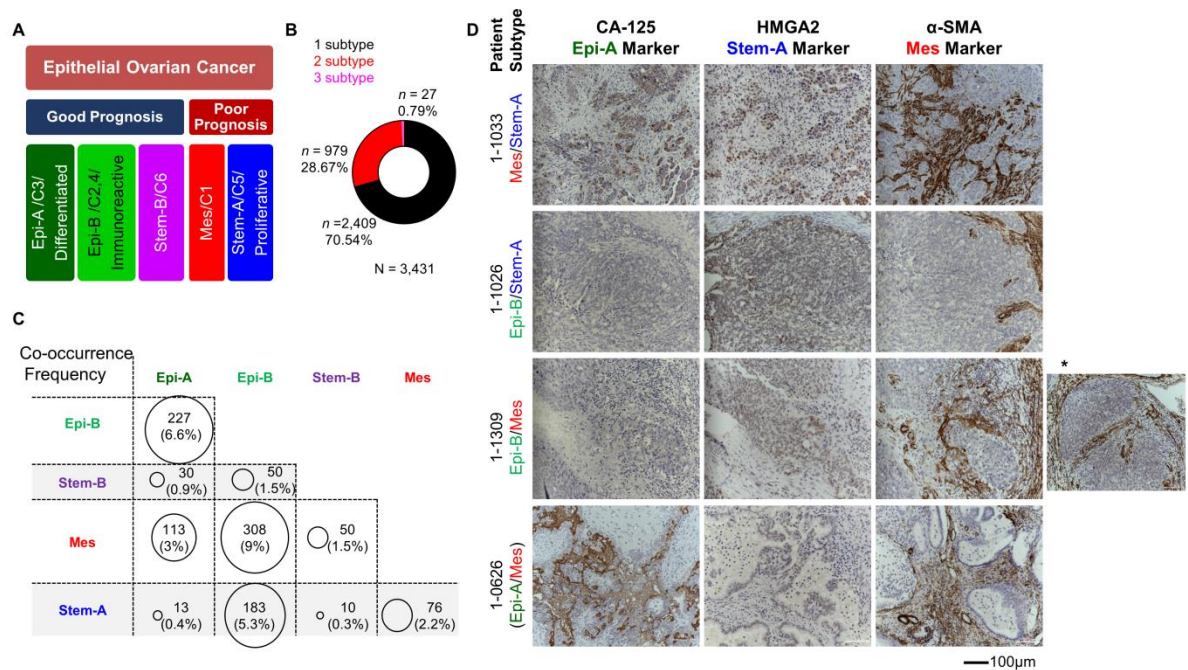
Figure 2. Correlation of tumour molecular subtype heterogeneity score and survival.

Kaplan-Meier analysis of overall- (A) and disease-free (B) survival in all samples with one subtype annotation (left panel), and stratified by ovarian cancer molecular subtypes (right panels). Significance is evaluated using log-rank test. Median of molecular subtype tumour heterogeneity score, an estimate of intra-tumoural heterogeneity, is used to separate the samples into high (black) and low groups (dotted line; grey colour). Percentage bar chart shows the composition of good prognosis subtypes (non-Mes/Stem-A%; black) and poor prognosis subtypes (Mes/Stem-A; grey) in tumour the molecular subtype heterogeneity-high and low groups. Significance evaluated using Fisher's Exact test. HR, hazard ratio.
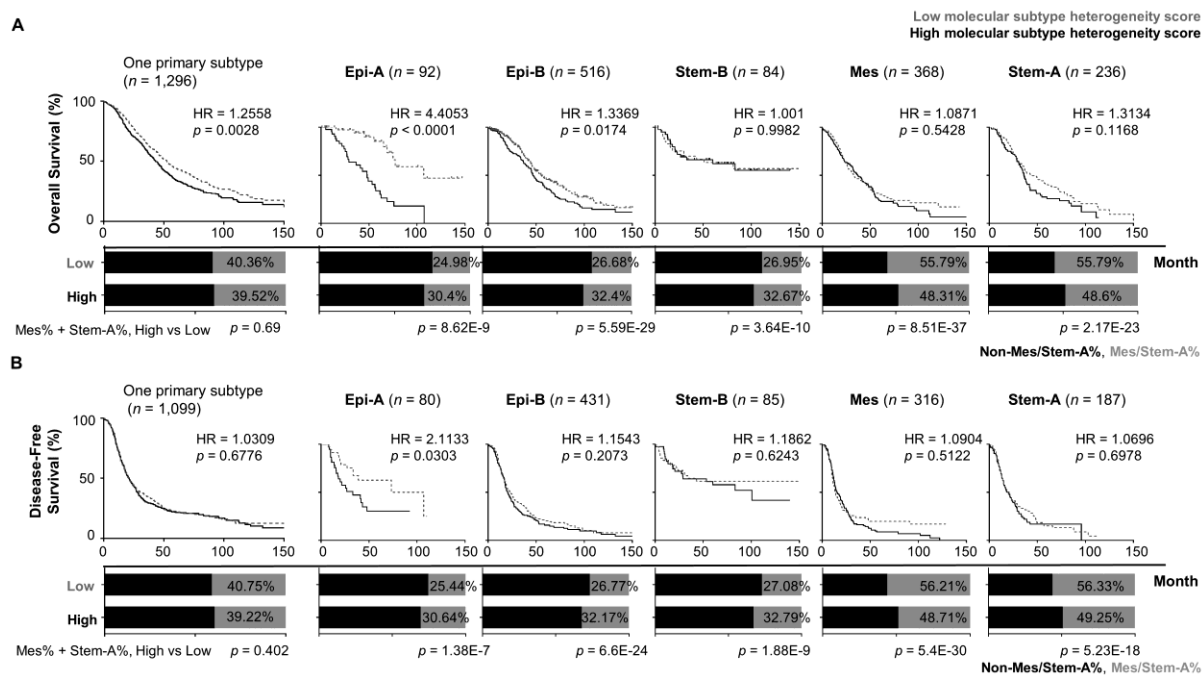
Figure 3. Molecular subtype composition is linked to clinical outcome in ovarian cancer.

(A) Dot plot of epithelial-mesenchymal transition (EMT) score (*y*-axis; mean±SEM) in various molecular subtype compositions (*x*-axis) found in ovarian cancer from CSIOVDB (*n* = 3,431). Significance is evaluated using Mann-Whitney test. Selected comparisons are shown.

(B) Kaplan-Meier analysis of overall- (upper panel) and disease-free (lower panel) survival stratified by molecular subtype compositions: Epi-A versus Epi-A/Mes (left); Epi-B versus Epi-B/Mes and Epi-B/Stem-A (middle); and Mes, Stem-A versus Mes/Stem-A (right). Significance is evaluated using log-rank test.

(C) Bar plot indicating the median overall Kaplan-Meier analysis of overall and disease-free survival in CSIOVDB (left panel), validation cohort (middle panel) and in ICGC-ACOS cohorts (right panel), where ovarian cancers are stratified into no (% = 0) or low (lowest 33%) Mes/Stem-A (green), partially (0 < % < 100) or intermediate (medium 33%) Mes/Stem-A (red), and fully (% = 100) or high (highest 34%) Mes/Stem-A (maroon). The *p*-value was computed by log-rank testing. HR, hazard ratio; OS, overall survival; DFS, disease-free survival

Subtype colour code: Epi-A, dark green; Epi-B, light green; Mes, red; Stem-A, blue; Stem-B, purple.
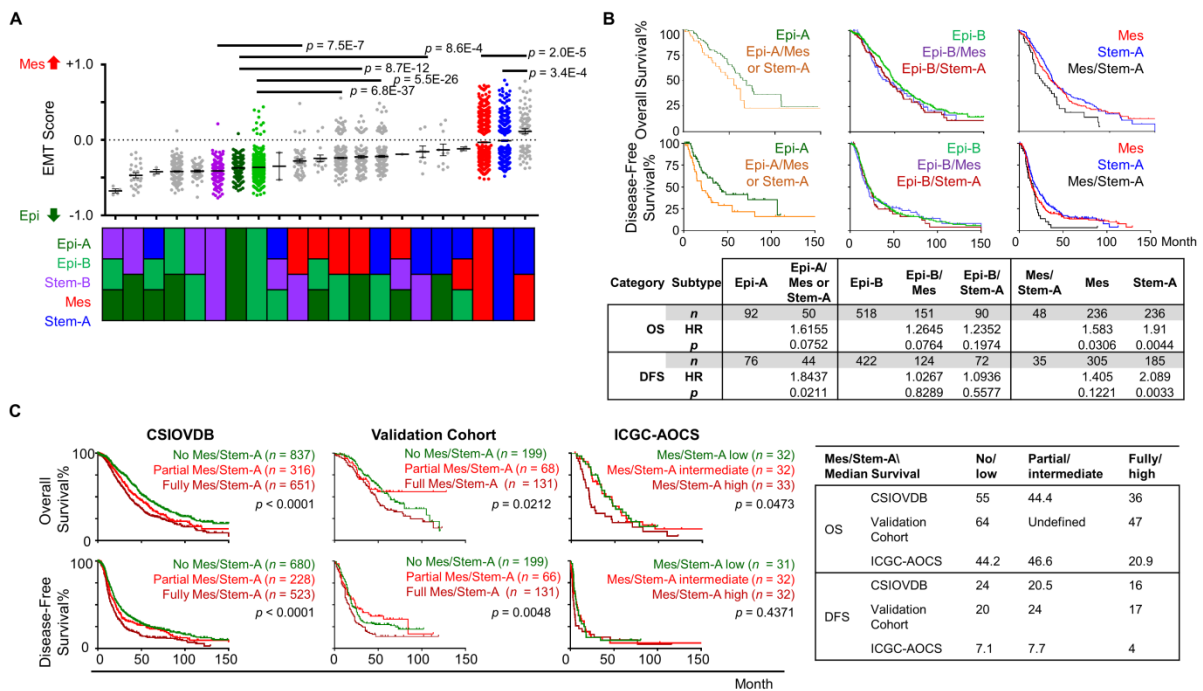

Figure 4. Ovarian cancer metastasis composed of predominantly Mes or Stem-A subtype.

(A) Bar plots showing the MASH percentage of primary ovarian cancer and metastasis (omental, peritoneal, or other distant) or ascites from five dataset. A bar plot showing the poor prognosis Mes and Stem-A subtypes composition percentage is shown each on the right of the MASH bar plots.

(B) Frequency plot of Mes and Stem-A percentage (% > 0, red; % = 0, black) within a tumour in primary and metastasis/relapsed ovarian cancer. The *p*-value was computed using Fisher's exact test.

(C) Heatmap showing the conditional probability of metastasis subtype given the primary subtype. Blue = low and red = high probability. Mets, metastasis; MASH, molecular assessment of subtype heterogeneity. Subtype colour code: Epi-A, dark green; Epi-B, light green; Mes, red; Stem-A, blue; Stem-B, purple.
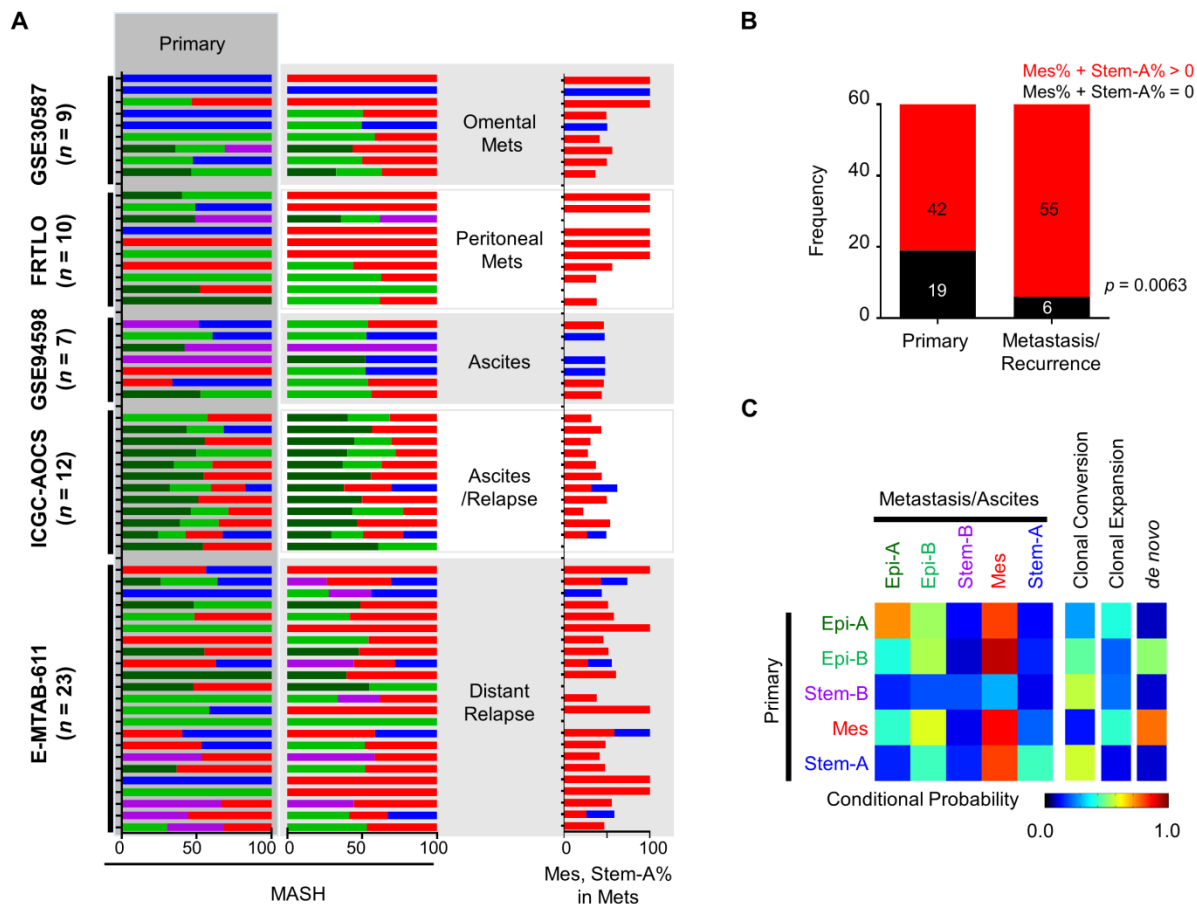
Figure 5. MASH implementation as clinical assay.

(A) Scheme of implementing MASH into a clinical assay.

(B) Comparison of MASH predictions from microarray and NanoString on training (left) and testing (right) dataset. Top colour bar indicates FFPE year (blue = young, yellow = old FFPE). Second colour bar indicates MASH label from microarray. Enrichment score heatmap shows MASH prediction from NanoString (blue = low; red = high).

(C) Classifier ROC curves of poor prognosis Mes, Stem-A and good prognosis subtypes Epi-A, Epi-B and Stem-B developed using FFPE samples from NUH testing cohort (*n* = 31) on NanoString. ES, enrichment score; ROC, receiver operative characteristic curve; AUC, area under the curve. Subtype colour code: Epi-A, dark green; Epi-B, light green; Mes, red; Stem-A, blue; Stem-B, purple.
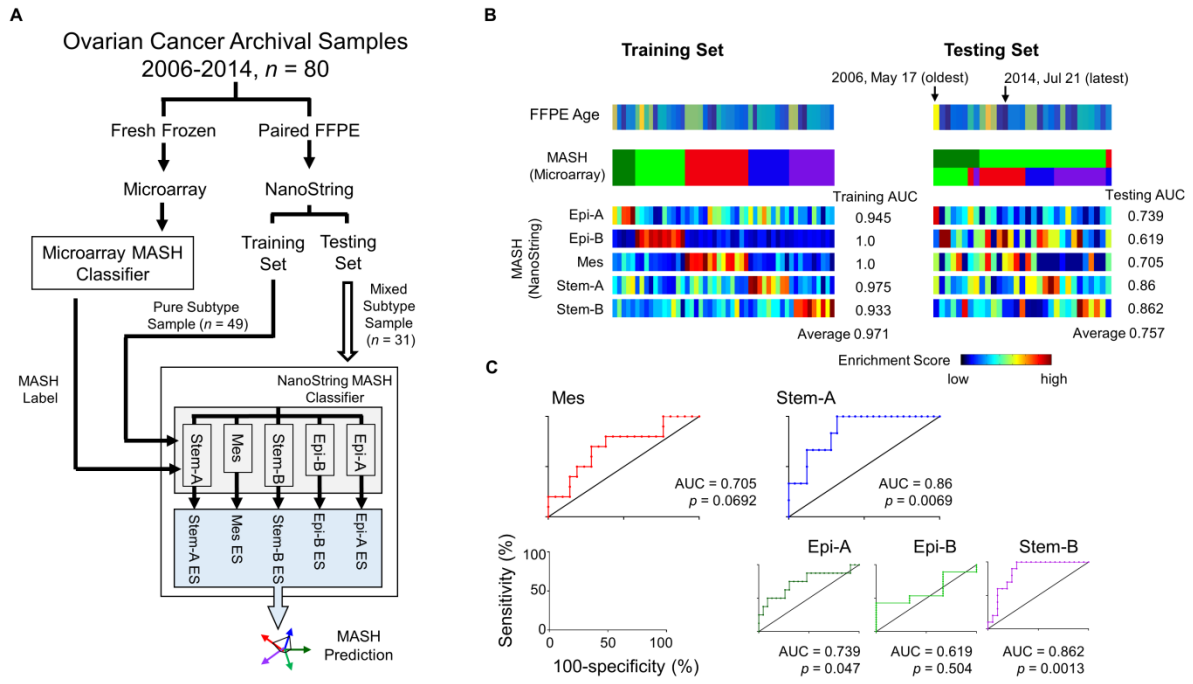
SUPPLEMENTARY MATERIAL ONLINE

Supplementary materials and methods YES

Supplementary figure legends YES

Figure S1. Molecular subtype predictor of ovarian cancer

Figure S2. Intra-tumour heterogeneity and histology of ovarian cancer

Figure S3. Validation of subtype-specific marker antibodies

Figure S4. Intra-tumour heterogeneity in ovarian cancer

Figure S5. Composition of poor prognosis subtypes confer poor ovarian cancer outcome in validation cohort

Figure S6. Percentage composition of Mes and Stem-A

Figure S7. MASH impact on drug treatment

Figure S8. Raw subtype enrichment scores in validation cohorts [Ed Note: mentioned in Suppl MandM file]

Table S1. Classification accuracy of MASH assay